Complete methane oxidation over Ba modified Pd/Al$_2$O$_3$: The effect of water vapor

Ida Friberg, Nadezda Sadokhina, Louise Olsson*

Chemical Engineering, Competence Centre for Catalysis, Chalmers University of Technology, SE-412 96 Gothenburg, Sweden

ABSTRACT

The effect on complete methane (CH$_4$) oxidation activity by an addition of up to 2 wt.% barium (Ba) promoter to alumina supported palladium (Pd/Al$_2$O$_3$, 2 wt.% Pd) was investigated. The catalyst samples were characterized with various techniques; temperature programmed oxidation (TPO), temperature programmed reduction with CH$_4$ (CH$_4$-TPR), X-ray photoelectron spectroscopy (XPS), scanning transmission electron microscopy (STEM) and *in situ* diffuse reflectance infrared Fourier transform spectroscopy (*in situ* DRIFTS). Flow reactor was used to investigate the CH$_4$ oxidation activity in the presence and in the absence of water vapor and also to evaluate the possibility to regenerate the catalytic activity after water vapor exposure. The results from the TPO and the CH$_4$-TPR experiments together with the XPS analysis gave no evidences for electronic promotion of the catalytic activity by addition of 0.5–2 wt.% Ba. This goes in line with the CH$_4$ conversion in dry gas condition, which was not affected by the Ba addition. However, we observed that an addition of Ba to Pd/Al$_2$O$_3$ enhances the CH$_4$ oxidation activity in the presence of water vapor, hence mitigates the effect of water deactivation. Interestingly, it was also seen that after water vapor exposure, the CH$_4$ oxidation activity could be regenerated to greater extent for the Ba promoted samples, particularly for the regeneration temperatures of 500–600 °C. Our results clearly show that the support influences the water deactivation of the active palladium sites and that the addition of barium is beneficial for the catalyst regeneration.

1. Introduction

Methane-based fuels, such as natural gas, are heavily used in different applications such as fuel for vehicles. Lean burn natural gas engines produces relatively low amounts of SO$_x$ and NO$_x$ as well as CO$_2$ compared to combustion of other fossil fuels [1]. However, incomplete combustion results in considerable emissions of CH$_4$ which has a significantly higher contribution to the greenhouse effect than an equal amount of CO$_2$. The increased awareness of global warning during the last decades has stressed the importance of limiting the emission of CH$_4$, which has resulted in a great effort to develop efficient catalysts for proper exhaust gas aftertreatment.

The highest activity for complete CH$_4$ oxidation can be obtained with palladium (Pd) based catalysts [2]. Palladium is typically supported upon metal-oxides with high surface area, such as γ-Al$_2$O$_3$. Several authors have observed that oxidized palladium (PdO) or PdO in combination with metallic palladium (Pd°), are most active for CH$_4$ oxidation at lower temperatures, whereas Pd° is the active phase at higher temperatures [3–7]. However, the activity of Pd/Al$_2$O$_3$ becomes severely inhibited by water [2,8] at temperatures below 450 °C [9].

Several authors have addressed this to formation of surface hydroxyl groups, which blocks active catalyst sites [9–12]. Another recent explanation is that the formed hydroxyl groups suppress oxygen exchange between support and PdO [13,14]. In a recent study [15] we found, based on experiments and kinetic modelling, that there are two routes for the water inhibition; rapid adsorption of water species on the active sites and also slow build-up of hydroxyl species. Moreover, high concentration of oxygen [16] and high concentration of water vapor [11] has also been found to facilitate formation of surface hydroxyls.

Several studies have shown that the water deactivation of Pd/Al$_2$O$_3$ is reversible. Persson et al. [17] reported that the initial activity of Pd/Al$_2$O$_3$ can be recovered by increasing the temperature to above 600 °C. They also showed that CH$_4$ oxidation activity of Pd/Al$_2$O$_3$ is easier to regenerate in air than in N$_2$ after water vapor exposure. Also Roth et al. [18] showed that the degree of regeneration depends on the temperature and close to full regeneration was achieved in He purge at 600 °C. Gao et al. [12] reported near to complete regeneration in N$_2$ flow at 550 °C whereas the catalyst could not be fully recovered at the same temperature in air. Moreover, Kikuchi et al. [11] regenerated the catalytic activity completely under lean condition between cyclic feeds of

---

water vapor at 280 °C.

Barium promoted Pd/Al_2O_3 has been investigated in several studies [19–23]. Alkaline earth metals, such as Ba, are electron donors and may therefore increase the electron density on the active metal surface, thus facilitate adsorption and desorption of oxidizing and reducing species, respectively [24]. This effect has previously been demonstrated for Ba promoted Pd/Al_2O_3 [20,22]. Also Thevenin et al. [21] observed electronic promotion for Ba doped Pd/Al_2O_3 after calcination at 1000 °C, whereas this effect could not be seen after gentler thermal treatment at 500 °C. Furthermore, addition of Ba has been found to stabilize the alumina to resist crystal phase transition at elevated temperatures from 1000 °C [21,23,25,26], hence also to preserve the high surface area of the support. It is suggested that Ba atoms incorporated in the Al_2O_3 lattice hinder the atomic diffusion driven transformation from γ-Al_2O_3 to δ-, θ- and α-Al_2O_3 [25]. Klingstedt et al. [20] showed that it was possible to retain higher CH_4 oxidation activity after hydrothermal ageing at 850 °C with a relatively high Ba content (15 wt.%) in Pd/Al_2O_3.

However, most of available literature is based on Ba promoted Pd/Al_2O_3 tested at dry gas conditions or for high temperature combustion application. To our knowledge there are no studies available that have examined the effect that Ba has on the water deactivation and regeneration of Pd containing catalysts. Therefore, the objective of the current work is to investigate the CH_4 oxidation over Pd/Al_2O_3 promoted with low amount of Ba, with a focus on water inhibition and the possibility to regenerate the catalyst. The catalyst system has been tested in flow reactor under various conditions to investigate deactivation limits and regeneration procedures and characterized with STEM, XPS, TPO, CH_4-TPR and DRIFTS.

2. Experimental

2.1. Catalyst preparation

Powder samples with 2 wt.% Pd content supported upon Al_2O_3 were prepared using wet impregnation method accompanied with freeze-drying. Al_2O_3 powder (Sasol, Puralox, SBa-200), calcined 2 h at 700 °C in air, was suspended in milliQ H_2O and pH was adjusted to 4 using dilute HNO_3. Palladium precursor ($Pd(NO_3)_2$, Heraeus GmbH) diluted with milliQ H_2O was added to the suspension and the pH was stabilized at 2. The slurry was frozen with liquid nitrogen and dried in vacuum during a prolonged period of time, at least 12 h, to assure complete water sublimation. The obtained catalyst powder was calcined 2 h at 550 °C in air.

Three samples of Pd/Al_2O_3 promoted with 0.5, 1 and 2 wt.% Ba were also prepared using wet impregnation method. A slurry was prepared from Pd/Al_2O_3 powder and milliQ H_2O and pH was stabilized at 4 with dilute HNO_3. Appropriate amount of $Ba(acetate)_2$ was dissolved in milliQ H_2O and added dropwise to the Pd/Al_2O_3 suspension. Diluted NH_3 solution was dripped into the slurry to adjust the pH to 8. The slurry was freezedried and calcined 2 h at 550 °C in air.

Monolith samples were prepared from catalyst powder deposited on cordierite monoliths (Ø = 21 mm, L = 20 mm, 400 cpsi). The empty monoliths were calcined at 600 °C for 2 h prior to washcoating. A slurry containing 20 wt.% solid content (4:1 ratio of catalyst powder to boehmite binder, Sasol Dispersal P2) and 80 wt.% liquids (1:1 ethanol to water) was prepared for each sample. The monolith was dipped into the slurry and dried in air at 100 °C for 4 min. This was repeated multiple times until the mass of washcoat reached 500 ± 10 mg. Thereafter, the wahscoated monoliths were calcined 2 min at 500 °C, followed by calcination in oven at 500 °C for 2 h.

2.2. Degreening, pretreatment and catalytic activity measurement in flow reactor

The catalytic activity was tested in flow reactor setup. The monolith

was put in a quartz tube (L = 800 mm, Ø = 21 mm) enclosed with a heating coil and wrapped in insulation. The temperature was controlled by an Eurotherm system and a thermo-couple positioned 10 mm upstream the monolith. Simultaneously, the catalyst temperature was monitored by a second thermo-couple, placed centrally in the monolith. The results herein presented, have been associated to the latter recorded temperature. The outside of the monolith was covered with quartz wool to avoid by-pass of gases. Desired inlet gas flow was obtained using multiple, individual MFC:s (Mass Flow Controllers, Bronkhorst). A CEM (Controlled Evaporation Mixing, Bronkhorst) system was used to evaporate and dose the water vapor. The concentrations of outlet gases were measured and monitored with an IR spectrometer (Fourier Transformed Infrared Spectroscopy, MKS MultiGas 2023 HS). For all experiments, Ar was used as inert carrier gas and the total flow velocity was 3500 mL min^{-1} (corresponding gas hourly space velocity: 30 000 h^{-1}), unless else is stated.

Prior to the experiments, the monoliths were subjected to a degreening procedure in order to stabilize the catalyst against changing during the activity test. The degreening procedure were performed as following: (1) reduction in 2 vol.% H_2 at 500 °C for 30 min; (2) lean conditions (500 ppm CH_4, 8 vol.% O_2 and 5 vol.% H_2O) at 700 °C for 60 min; (3) rich condition (2 vol.% H_2 and 5 vol.% H_2O) at 700 °C for 20 min; followed by repetition of the step (2). Each monolith was degreened once before the first experiments. Prior to each experiment, the monoliths were also pre-treated in 8 vol.% O_2 at 700 °C for 30 min or 60 min. The methane oxidation activity was tested using a gas mixture of 500 ppm CH_4 and 8 vol.% O_2 ('dry reaction mixture') or 500 ppm CH_4, 8 vol.% O_2 and 5 vol.% H_2O ('wet reaction mixture').

The first activity test will be referred to as the 'ramping test'. Prior to the ramping test, the monoliths were pre-treated during 30 min in 8 vol.% O_2 at 700 °C, followed by cooling in Ar down to 150 °C. After this point, the temperature was increased (5 °C /min) to 700 °C in dry reaction mixture. The temperature was stabilized during 15 min followed by cooling to 150 °C (5 °C /min), in a continuous flow of dry reaction mixture. This cycle was repeated 3 times, without any pre-treatment between the ramps. The ramping test was also performed but with wet reaction mixture, *i.e.* all 3 cycles were conducted in the presence of 5 vol.% H_2O. The experiment performance was otherwise identical and is referred to as the ramping test in wet reaction mixture.

In the second activity test (referred to as the 'regeneration test'), the methane oxidation activity was tested in the presence of water vapor repeatedly followed by regeneration in H_2O and O_2 or only in O_2, at different temperatures. Prior to these experiments the catalysts were pre-treated in 8 vol.% O_2 at 700 °C for 60 min. The regeneration test consisted of two repeated steps, (1): exposure to wet reaction mixture at 450 °C for 3 h; (2): regeneration at X °C (X = 700/600/500 °C, in the current order). Thus the entire experiment was performed accordingly: (1) - (2) X = 700 °C - (1) - (2) X = 600 °C - (1) - (2) X = 500 °C - (1). Furthermore, the regeneration sequence, (2), can be explained in following steps, (2a): linear temperature ramp in Ar during 12.5 min to X °C; (2b): temperature stabilization in Ar for 10 min; (2c): exposure to 8 vol.% O_2 and 5 vol.% H_2O for 15 min at X °C; (2d): linearly ramped cooling during 50 min to 450 °C in 8 vol.% O_2 and 5 vol.% H_2O; (2e): temperature stabilization at 450 °C in 8 vol.% O_2 and 5 vol.% H_2O for 10 min. Subsequently, the catalyst was pre-treated once again in 8 vol.% O_2 at 700 °C for 60 min and the experiment was repeated but in the absence of water during the steps (2c), (2d) and (2e), so-called regeneration in O_2. The CH_4 conversion for the regeneration experiments are presented as the moving average within a 5 min time window.

2.3. Catalyst characterization

Before the characterizations, the fresh catalyst powder was placed in a ceramic beaker, and the ceramic beaker was placed in the flow reactor. This powder was degreened according to the degreening procedure described in Section 2.2, but with lower total gas flow, in this

case 2500 mL min^{-1}. After degreening, the powder was oxidized at 700 °C for 30 min in 8 vol.% O_2 and cooled to room temperature in Ar, also in the flow reactor.

2.3.1. Temperature programmed oxidation (TPO) and temperature programmed reduction (TPR)

TPO and CH_4-TPR were performed in a Differential Scanning Calorimeter (Sensys DSC, Setaram). The gas feed was controlled by multiple MFC:s (Bronkhorst) and a mass spectrometer (Hiden HPR-20 QUI MS) was used for detection of the exiting gases with the *m/e* ratios of 44 (CO_2), 32 (O_2), 28 (CO), 15 (CH_4) and 2 (H_2). The sample powder was weighed to 60 mg and put upon a porous, sintered quartz bed inside a vertical quartz tube (Ø = 5.0 mm). The total flow was fixed at 20 mL min^{-1} and Ar was used as inert carrier gas. First, the catalyst powder was pre-reduced in 2 vol.% H_2 at 500 °C for 30 min and cooled (5 °C /min) to room temperature (RT) under the same reducing conditions. The catalyst powder was flushed with 1500 ppm O_2 at RT for 20 min. A rather low oxygen concentration was used in order to more clearly observe the consumed oxygen. Subsequently, the TPO was conducted by ramping temperature (10 °C /min) up to 700 °C, followed by temperature stabilization for 20 min and cooling (10 °C /min). The inlet concentration of O_2 was kept constant at 1500 ppm during the entire TPO sequence.

Prior to the consecutive CH_4-TPR, the catalyst powder was pre-oxidized in 5 vol.% O_2 while the temperature was kept constant at 500 °C for 30 min and thereafter decreased (5 °C /min) to RT, also in O_2. The CH_4-TPR was performed with 1500 ppm CH_4, first at RT for 20 min and thereafter the temperature was increased (10 °C /min) to 700 °C, also with a constant inlet concentration of 1500 ppm CH_4.

2.3.2. Scanning transmission electron spectroscopy (STEM)

The catalyst surface was imaged with scanning transmission electron microscope (STEM) to acquire an overview of the surface as well palladium particle shape and size distribution. Degreened catalyst powder was finely grinded in a mortar and distributed on a carbon copper TEM grid. For the analysis, FEI Titan 80–300 equipped with probe Cs-corrector and high-angle annular dark-field (HAADF) detector, was used. The microscope was operated with a voltage of 300 kV and scanning mode (STEM) was used for imaging. EDXS (Energy Dispersive X-ray Spectroscopy) analysis was performed on several areas for elemental analysis.

2.3.3. In situ diffuse reflectance infrared fourier transform spectroscopy (DRIFTS)

In order to produce high quality DRIFTS spectra, the catalyst powder was diluted with non-absorbing KBr and powder particle size distribution was narrowed by sieving. Degreened powder was mixed with 10 wt.% KBr and compressed into a pellet. The pellet was pestled into powder with a mortar and the powder fraction in the size range of 40–80 μm was separated and used for analysis. Spectra with wave numbers 400–4000 cm^{-1} and resolution of 4 cm^{-1} were collected using a Vertex 70 spectrometer (Bruker) with a MCT detector, cooled with liquid nitrogen. The sample was put in stain-less steel reaction chamber (Praying Mantis, High Temperature Reaction Chamber) equipped with water resistant CaF_2 windows. The sample bed temperature was measured using a thermo-couple and regulated with a Eurotherm system. All the gases were dosed and controlled by several MFC:s (Bronkhorst) and the water vapor was obtained and dosed from a CEM system (Bronkhorst).

The total gas flow in the reaction chamber was regulated to 50 mL min^{-1} and the temperature was kept constant at 550 °C, for all steps in all experiments. Prior to each experiment, the samples were pre-treated in 2 vol.% O_2 for 60 min. The first experiment was followed by 120 min exposure to 1 vol.% water vapor and 2 vol.% O_2. The background spectra was collected in the end of this step. Subsequently, spectra were recorded simultaneously as the chamber was provided

with a water free gas feed containing 2 vol.% O_2 during 120 min. The oxidative pre-treatment was repeated prior to the second experiment and the background spectra was collected in the end of this step. Thereafter spectra collection was started and the chamber was fed with 1 vol.% water vapor and 2 vol.% O_2 in Ar for 120 min followed by a dry gas feed with 2 vol.% O_2 for 180 min.

2.3.4. X-ray photoelectron spectroscopy

XPS (X-ray Photoelectron Spectroscopy) was performed in ultrahigh vacuum using a Perkin Elmer PHI 5000C ESCA system equipped with monochromatic Al Kα X-ray source with the binding energy of 1486.6 eV. For reference, the C1s with a binding energy of 284.6 eV was used. Degreened powder was pressed firmly upon a carbon rubber pads attached to the sample holder, before inserting into the instrument.

3. Results and discussion

3.1. Catalyst characterization

Catalyst powder, previously degreened and oxygen pre-treated at 700 °C, was analyzed with STEM. The images reveal clearly separated and well distributed Pd particles, see Fig. 1. The mean Pd particle diameter was estimated to around 8–9 nm for the samples, by measurements of 100 individual particles per sample, see Table 1. It is expected that some sintering into larger particles would have occurred during the preceding high temperature degreening and pre-treatment procedure. However, the Pd particle mean diameter difference amongst the samples was no larger than 0.8 nm, which is not large enough to be significant. Thus, the Pd particle size appears to be similar for all samples, *i.e.* an addition of Ba did not show any effects to prevent Pd particle sintering, which also has been reported previously [21]. Low amount of Ba was detected for the promoted samples with EDXS analysis. However, despite investigation of several areas of the catalyst, both with high and low Pd content, no remarkable high concentrations of Ba were localized. Hence, Ba is believed to be well dispersed over the catalyst material.

The possible promoting effect of Ba was studied with TPO and CH_4-TPR. Addition of electronic promoters, such as Ba, may by virtue of electron donation change the electron density and thus facilitate for instance adsorption of oxygen. Fig. 2 shows the outlet concentration of O_2 in relation to catalyst bed temperature obtained in the TPO experiment. The maximum O_2 oxidation occurred at around 339 °C for all the samples which is shown by the O_2 consumption peak. Thevenin et al. [21] reported TPO results with maximum O_2 adsorption at around 300 °C for Pd/Al_2O_3 and Pd/Al_2O_3 promoted with 3 wt.% Ba, thus similar to our results. Also, minor decomposition of PdO into metallic Pd was observed by a slightly increased O_2 concentration at the highest temperature (700 °C). The TPO profiles were almost identical for all the samples, indicating that a concentration of 2 wt.% Ba might not be high enough to benefit from an effect of electronic promotion.

Neither any clear differences were found among the samples in the CH_4-TPR patterns, displayed in Fig. 3. The CH_4 consumption peak at around 202 °C occurred simultaneously as a sharp peak of CO_2 formation appeared, see Fig. S1–S4 presented in Supplementary Materials. This is due to reduction of PdO with CH_4 which results in H_2O and CO_2 production [16,27,28]. From around 380 °C and up, a steady decrease in CH_4 concentration was seen, simultaneously as H_2, CO and CO_2 were formed, also shown in Fig. S1–S4 in Supplementary Materials. This is associated to *(i)* steam reforming reaction, where CH_4 reacts with adsorbed H_2O to form CO and H_2, *(ii)* water gas shift reaction, where CO is further reacted with adsorbed H_2O to form CO_2 and H_2 [16,27,28] and *(iii)* surface coke formation with production of H_2 [16,27]. Moreover, since only very small amounts of water could be detected, most of the produced H_2O was likely adsorbed on catalyst surface.

In addition, the oxidation state of Pd was verified with XPS analysis, displayed in Fig. 4. All samples exhibited doublets with peak maxima at
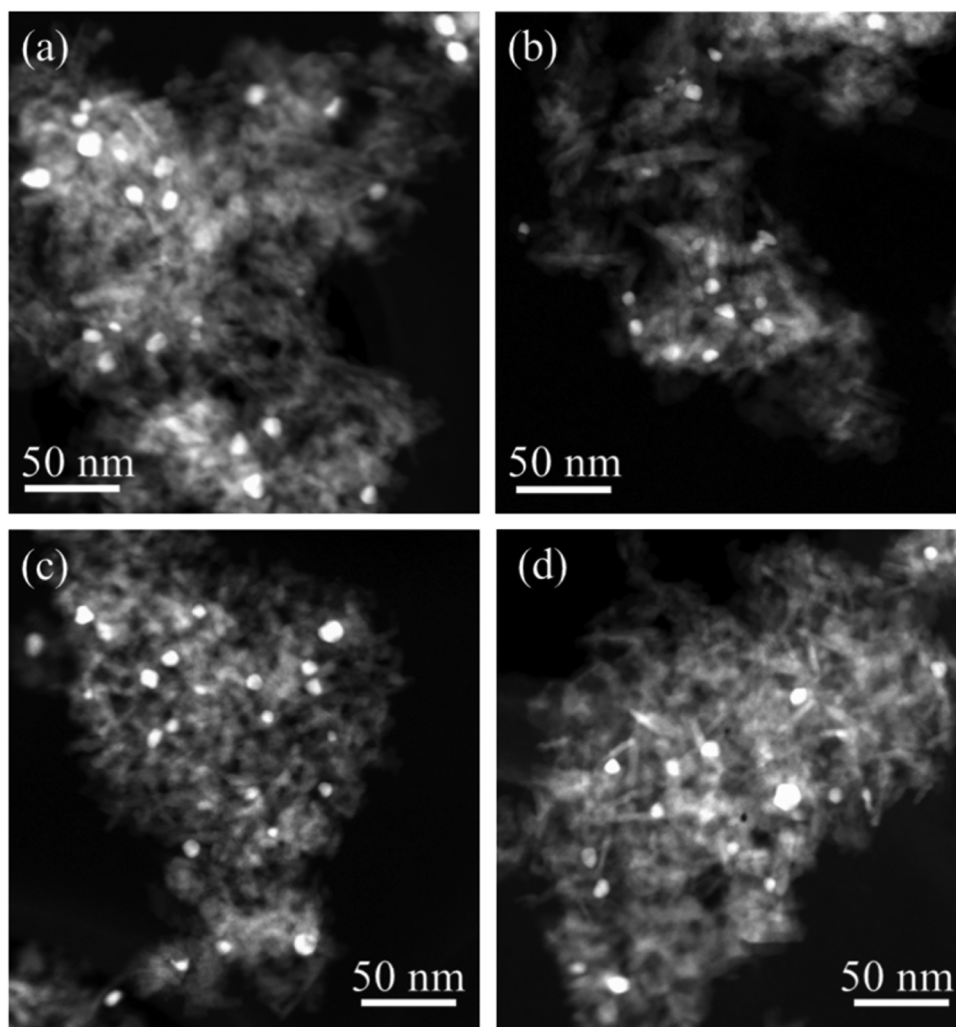
Fig. 1. STEM images of (a) PdAl, (b) PdAl-0.5Ba, (c) PdAl-1Ba and (d) PdAl-2Ba. The catalyst powders were degreened in flow reactor, see Section 2.3, prior to the STEM analysis.

Table 1
List of all prepared samples with respective Ba content together with mean Pd particle diameter with corresponding standard deviation.

	Ba content, wt.%	Pd particle mean diameter[*], nm (σ^*, nm)
PdAl	0	9.0 (2.3)
PdAl-0.5Ba	0.5	8.4 (2.3)
PdAl-1Ba	1	8.7 (1.9)
PdAl-2Ba	2	8.2 (1.9)

* Estimated from STEM images.

335.2 eV and 340.45 eV, which correspond to the binding energy of the $3d_{5/2}$ and $3d_{3/2}$ electrons in metallic Pd (Pd°), respectively [29,30]. The binding energy of the $3d_{5/2}$ electrons in oxidized Pd has been reported to 336.7 eV for Pd^{2+} [29,31] and 337.9 eV for Pd^{4+} [32]. Thus, the slightly asymmetric peak shapes indicate presence of PdO and possibly also PdO_2, although in smaller proportions than Pd°. It should be noted that PdO_2 has been observed in several XPS studies [29,33,34] even though it is an unstable compound in dry conditions [29]. A suggested explanation for this is stabilizing interactions with the support material in high vacuum [29]. Ba induced electronic promotion would have been indicated by shifted binding energies of the Pd3d electrons towards higher oxidation states [21]. Another possibility is that the interaction with Ba could result in increased electron density around PdO, which consequently appears as Pd° at lower binding energies in the XPS spectra [20,35]. However, the binding energy of the Pd3d electrons
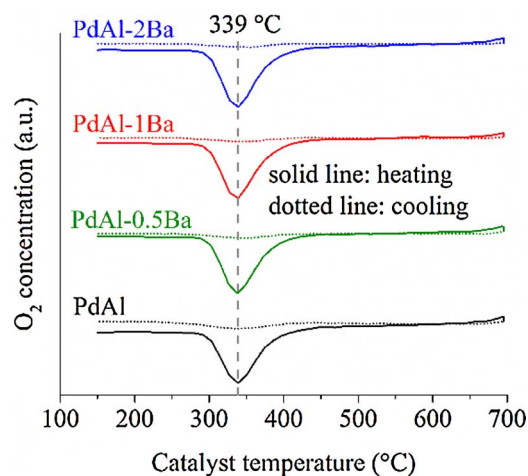

Fig. 2. Outlet O_2 concentration during TPO experiments. From top to bottom: PdAl-2Ba (blue line), PdAl-1Ba (red line), PdAl-0.5Ba (green line) and PdAl (black line). The fresh catalyst powders were degreened in flow reactor, see Section 2.3, prior to the TPO. (For interpretation of the references to colour in this figure caption, the reader is referred to the web version of this article).

were similar for all samples (Fig. 4). Thus, these results agree well with the TPO and CH_4-TPR data (Figs. 2 and 3), *i.e.* no evidences for electronic promotion could be demonstrated for Pd/Al_2O_3 with an addition
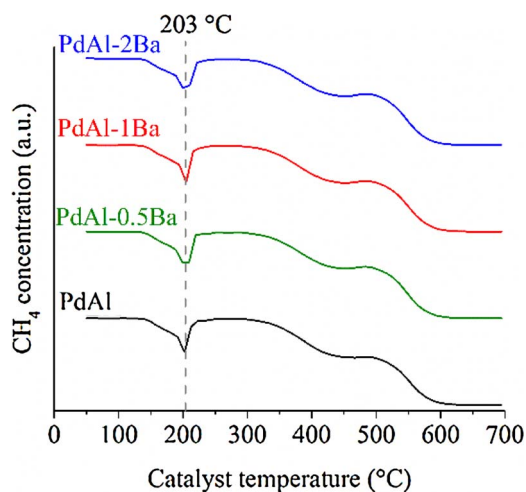
Fig. 3. Outlet CH_4 concentration during CH_4-TPR experiments. From top to bottom: PdAl-2Ba (blue line), PdAl-1Ba (red line), PdAl-0.5Ba (green line) and PdAl (black line). The fresh catalyst powders were degreened in flow reactor, see Section 2.3, prior to CH_4-TPR. (For interpretation of the references to colour in this figure caption, the reader is referred to the web version of this article).
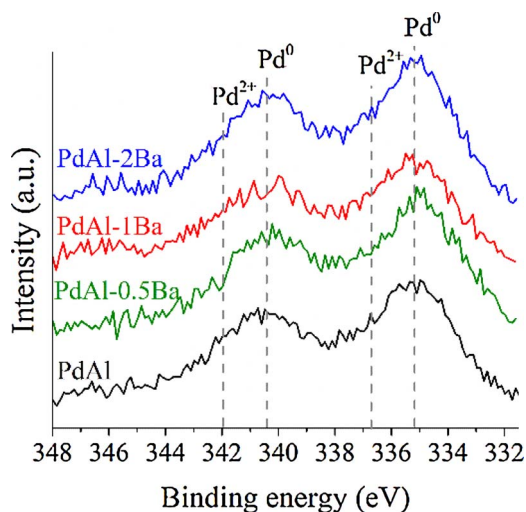

Fig. 4. XPS spectra for Pd3d. From top to bottom: PdAl-2Ba (blue line), PdAl-1Ba (red line), PdAl-0.5Ba (green line) and PdAl (black line). The catalyst powders were degreened in flow reactor, see Section 2.3, prior to the XPS analysis. (For interpretation of the references to colour in this figure caption, the reader is referred to the web version of this article).

of up to 2 wt.% Ba.

3.2. Methane oxidation activity in the absence of water vapor

The catalytic activity for CH_4 oxidation was evaluated in flow reactor using cordierite monoliths washcoated with catalyst powder and bohemite binder. The ramping test was performed by increasing and decreasing the temperature linearly, up and down between 150 and 700 °C. This was repeated three times, i.e. three cycles were performed. The results for the ramping test in dry reaction mixture, for PdAl and PdAl-2Ba, are displayed in Fig. 5. It can be seen that the activity was rather similar for both samples when no water vapor was present in the gas feed, where $T_{50\%}$ (temperature of 50% CH_4 conversion) ranged between 272–283 °C, see Table 2. Thus, such small differences in $T_{50\%}$ are not significant. This observation goes in line with the previously discussed results, where it was discovered that the Ba addition introduces no or very little electronic promotion. Both samples exhibited some hysteresis in cycle 1, expressed as slightly higher $T_{50\%}$ during the
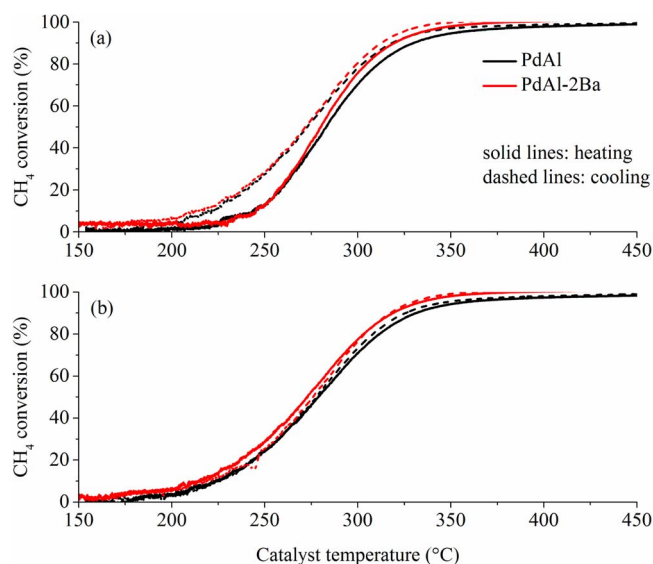

Fig. 5. Methane conversion during ramping test in dry reaction mixture (500 ppm CH_4, 8 vol.% O_2) for PdAl (black line) and PdAl-2Ba (red line). (a) presents cycle 1 and (b) cycle 2. The solid lines represent heating and dashed lines refer to cooling. (For interpretation of the references to colour in this figure caption, the reader is referred to the web version of this article).

heating ramp compared to the cooling ramp. This is particularly prominent in the temperature region 200–270 °C, Fig. 5a. In the TPO experiment (Fig. 2) we observed that only minor decomposition of PdO occurs at temperatures below 700 °C. Thus, a possible explanation for the hysteresis is that the excessive amounts of O_2 results in formation an highly active PdO phase during heating which also remains during cooling since the temperature does not exceed 700 °C. Furthermore, no hysteresis was observed during cycle 2 (Fig. 5b). This observation indicates that the catalyst stabilizes with time due to the formation of a stable PdO/Pd phase. It should also be noted that cycle 3 (not shown) was almost identical to cycle 2, for both samples.

3.3. The effect of water vapor on the methane oxidation activity

The same experiment (ramping test) was also performed with wet reaction mixture, i.e. with additional 5 vol.% water to the gas feed. These results are presented in Fig. 6. Compared to the previously discussed results of the ramping test conducted in dry reaction mixture, the $T_{50\%}$ were considerable higher here. Numerous of studies have agreed upon that water vapor deactivates Pd/Al$_2$O$_3$ [2,8], hence this is considered to be the reason for the higher light-off temperature. Another noteworthy trend, is that the water deactivation becomes more severe with time, expressed as gradually deteriorated catalytic activity for each cycle.

The results from cycle 1 are depicted in Fig. 6a and $T_{50\%}$ for all samples are presented in Table 2. All samples expressed similar activity during the first heating ramp, whereas the samples exhibited different catalytic activity during the cooling ramp. The highest activities were obtained with PdAl-0.5Ba and PdAl-1Ba, which demonstrated a $T_{50\%}$ of 431 °C and 427 °C, respectively, during cooling. Moreover, PdAl-2Ba also showed higher activity compared to the unpromoted PdAl. For these samples, the observed $T_{50\%}$ were 447 °C and 468 °C, respectively, during cooling. Interestingly, the CH_4 oxidation occurred at higher temperatures during the cooling ramp. There are different possible reasons for this hysteresis. It was seen in the TPO (see Fig. 2) that PdO is fairly stable at temperatures up to 700 °C, which also other authors have reported [16,27,33,36]. Therefore, decomposition of PdO into metallic Pd is not considered to be a probable reason for the activity drop during the cooling ramp. Furthermore, it could be suspected that some sintering would occur at the high temperature and consequently

Table 2
Temperature of 50% methane conversion ($T_{50\%}$) for the ramping test in dry and wet reaction mixture.

		PdAl (°C)	PdAl-0.5Ba (°C)	PdAl-1Ba (°C)	PdAl-2Ba (°C)
Dry reaction mixture	Cycle 1, heating	283	–	–	280
	Cycle 1, cooling	273	–	–	272
	Cycle 2, heating	279	–	–	273
	Cycle 2, cooling	278	–	–	276
Wet reaction mixture	Cycle 1, heating	401	397	394	400
	Cycle 1, cooling	468	431	427	447
	Cycle 2, heating	517	462	454	500
	Cycle 2, cooling	510	487	482	504
	Cycle 3, heating	543	531	530	558
	Cycle 3, cooling	522	513	510	522
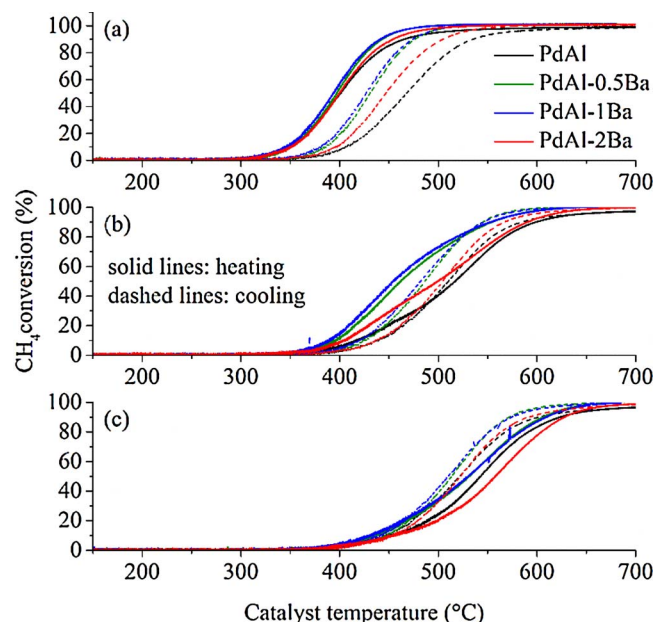
Fig. 6. Methane conversion during ramping test in wet reaction mixture (500 ppm CH_4, 8 vol.% O_2, 5 vol.% H_2O) for PdAl (black line), PdAl-0.5Ba (green line), PdAl-1Ba (blue line) and PdAl-2Ba (red line). (a) presents cycle 1, (b) cycle 2 and (c) cycle 3. The solid lines represent heating and dashed lines refer to cooling. (For interpretation of the references to colour in this figure caption, the reader is referred to the web version of this article).

result in decreased activity. However, since all samples already had been treated at 700 °C under lean and rich condition together with water vapor during the degreening and pre-treatment, this is neither believed to induce the hysteresis. Hence, the most reasonable explanation for this is rather that formation of surface hydroxyls is responsible for the activity loss during the cooling ramp [19,27].

Cycle 2 was also characterized by low $T_{50\%}$ for PdAl-0.5Ba and PdAl-1Ba whereas PdAl demonstrated the highest $T_{50\%}$, see Fig. 6b. This was also observed for the cycle 3, see Fig. 6c, with an exception of PdAl-2Ba which showed the highest $T_{50\%}$ among the samples during the heating ramp. Interestingly, the conversion lines for the heating and cooling ramps intersects during cycle 2. Furthermore, higher activity was obtained at cooling than at heating during cycle 3, which is the opposite to the results of cycle 1. This change of the hysteresis nature is also likely to be related to the hydroxyl-build up on the catalyst surface.

In this experiment, the gradually increased $T_{50\%}$ indicates that hydroxyl species, which are stable at temperatures up to 700 °C, were formed in the presence of water vapor. This has previously been ascribed to slow accumulation of hydroxyls on the catalyst surface [15] and was suggested to be facilitated by the high O_2 concentration [16]. Interestingly, it appears that with a low Ba content, this accumulative hydroxyl build-up is delayed, since the water deactivation effect

progresses slower over the three tested cycles. Thus, the Ba promoted samples demonstrated increased resistance against water deactivation. As an example, it could be mentioned that the difference in $T_{50\%}$ for PdAl and PdAl-1Ba for the heating ramp in cycle 2 was as much as 63 °C. Hence, from these experiments, 0.5–1 wt.% Ba appears to be most beneficial to retain the catalytic activity in the presence of water vapor. Possible reasons for this shown effect could be that Ba influences the availability of active catalyst sites and/or facilitate re-oxidation of the Pd as a result of: *(i)* weaker surface hydroxyl bonds which enhances dehydroxylation at lower temperatures and/or *(ii)* formation of different surface compounds.

Another experiment (regeneration test) was conducted in order to investigate the potential to regenerate the catalytic activity after exposure to water, *i.e.* to remove hydroxyl species from the catalyst surface. The regeneration steps were conducted at different elevated temperatures (700, 600 and 500 °C) and together with 5 vol.% H_2O and excessive levels of O_2. The catalytic activity was tested in wet reaction mixture between the regeneration steps and the corresponding CH_4 conversion is displayed in Fig. 7. It can be seen that the initial CH_4 conversion was 100% for all samples. However, already after 3 h exposure to the wet reaction mixture, all four samples showed a significant drop in conversion, however, to lesser extend for the Ba containing samples. Most activity loss was seen for PdAl followed by PdAl-0.5Ba, PdAl-2Ba and PdAl-1Ba, which showed the highest conversion. The same trend was also observed during the remaining steps of experiment. As expected, the regeneration temperature was a crucial parameter in order to remove the adsorbed hydroxyl species and regain the catalytic activity, which also has been reported in literature previously [17,18]. It should be noted that the heating to the regeneration
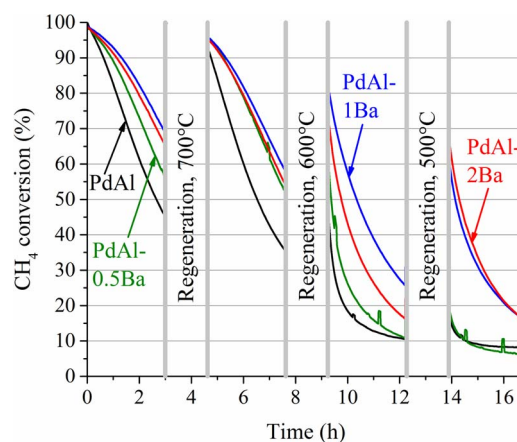
Fig. 7. Methane conversion in wet reaction mixture (500 ppm CH_4, 8 vol.% O_2, 5 vol.% H_2O) with wet regeneration (5 vol.% H_2O, 8 vol.% O_2) at 700, 600 and 500 °C in between, shown for PdAl (black line), PdAl-0.5Ba (green line), PdAl-1Ba (blue line) and PdAl-2Ba (red line). It should be noted that heating to the regeneration temperature was done in Ar only. (For interpretation of the references to colour in this figure caption, the reader is referred to the web version of this article).
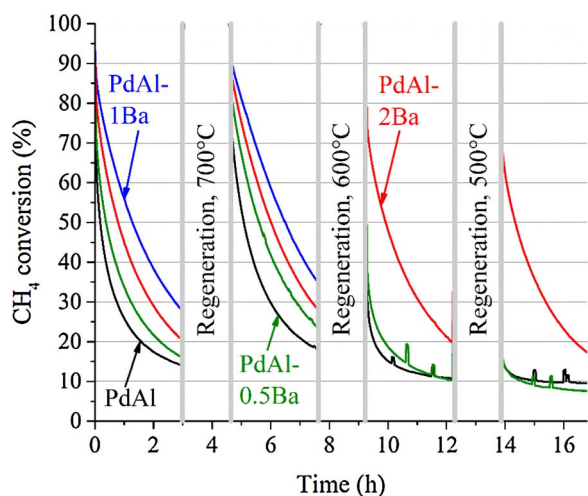
Fig. 8. Methane conversion in wet reaction mixture (500 ppm CH_4, 8 vol.% O_2, 5 vol.% H_2O) with dry regeneration (8 vol.% O_2) at 700, 600 and 500 °C in between, shown for PdAl (black line), PdAl-0.5Ba (green line), PdAl-1Ba (blue line) and PdAl-2Ba (red line). (For interpretation of the references to colour in this figure caption, the reader is referred to the web version of this article).

temperature was done in Ar only. Thus, during this heating it is likely that some hydroxyl species were removed. The activity of the un-promoted PdAl was rather efficiently recovered after regeneration at 700 °C. However, a significant drop in conversion was seen after regeneration at 600 °C and regeneration at 500 °C *i.e.* almost no regeneration effect was achieved. On the contrary, regeneration at 600 °C was much more efficient for PdAl-1Ba and PdAl-2Ba and interestingly, regeneration at 500 °C was almost as efficient for these two samples. In the first part of the experiment, PdAl-0.5Ba showed a conversion close the other Ba samples, but it could not be successfully regenerated at 600 and 500 °C. This findings also imply that there is a strong correlation between the Ba concentration and the resistance towards water deactivation, which was discussed previously.

The 60 min long dry O_2-pretreatment at 700 °C was repeated and followed by the same experimental procedure but with dry regeneration in O_2, see Fig. 8. First, it should be clarified that for none of the samples, the initial activity was completely regenerated during the dry pre-treatment. This is obvious by comparison of the first 3 h in Figs. 7 and 8. This observation further strengthen the indication highly stable hydroxyl species were formed. However, this experiment shows similar trends as the previous regeneration experiment. Least water deactivation was seen for PdAl-1Ba and PdAl-2Ba and lowest CH_4 conversion was obtained with PdAl-0.5Ba and unpromoted PdAl. Also sensitivity towards the regeneration temperature was shown. As in previous experiment, PdAl appears to be difficult to regenerate at lower temperatures (600 and 500 °C) whereas PdAl-2Ba was significantly better regenerated at these temperatures.

The regeneration tests showed that an addition of Ba to Pd/Al_2O_3 improves the resistance against water deactivation, which agrees with the results of the wet ramping test (Fig. 6). The effect is particularly evident when regeneration at lower temperatures (600 and 500 °C) were tested. Here, considerable less activity was regenerated for PdAl compared to PdAl-1Ba and PdAl-2Ba (Figs. 7 and 8). This implies that the less stable hydroxyl groups are formed on the catalyst surface of the Ba promoted samples compared to the unpromoted PdAl samples.

3.4. Formation of surface hydroxyl species

In situ DRIFTS experiments were performed to further investigate the effect of water and surface hydroxyl formation on PdAl and the sample with the highest Ba content, *i.e.* PdAl-2Ba. In the first experiment, the samples were pre-treated in 2 vol.% O_2 at 550 °C and
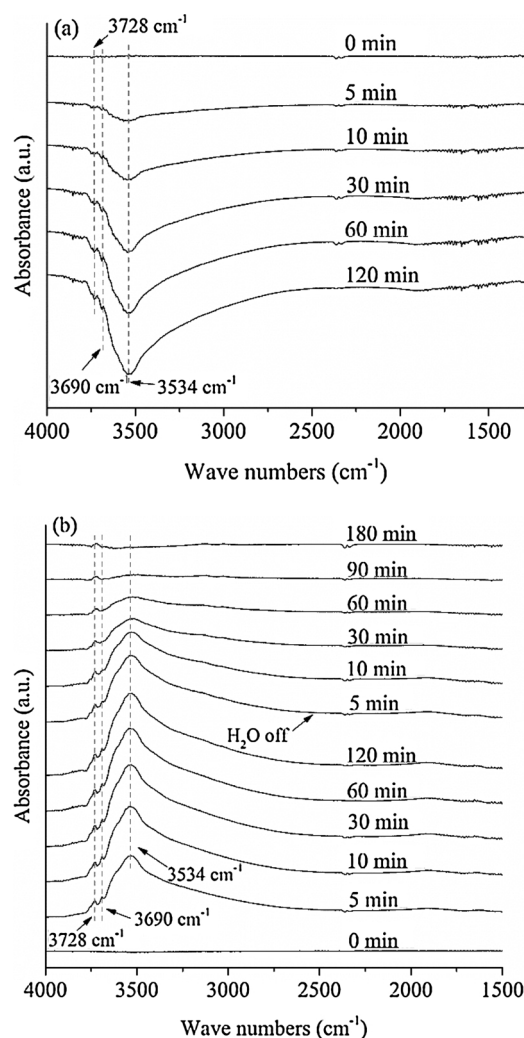

Fig. 9. *In situ* DRIFTS spectra for desorption/adsorption of water/hydroxyls on the surface of PdAl at 550 °C. The spectra were collected during (a) 120 min O_2/Ar purge after H_2O_g/O_2/Ar exposure, the background was acquired with presence of H_2O_g/O_2 and (b) during 120 min H_2O_g/O_2/Ar exposure followed by 180 min of O_2/Ar purge, the background was acquired with presence of O_2.

subsequently flushed with 2 vol.% O_2 and 1 vol.% water vapor in Ar for 120 min at 550 °C. The background spectrum was acquired in the end of this step, *i.e.* with water vapor and O_2 present. The spectra presented in Figs. 9a and 10a were collected during the consecutive O_2/Ar purge and consequently, the negative peaks represent the dehydroxylation of the catalyst surface of respective sample. Prior to the next experiment, the oxidizing pre-treatment was repeated and a new background spectrum was acquired in the end of this step, *i.e.* in dry O_2/Ar flow. The bottom spectra in Figs. 9b and 10b show the subsequent 120 min of 1 vol.% water vapor and 2 vol.% O_2 exposure and hydroxyl build-up. The water vapor was thereafter removed and the gradual desorption of hydroxyl species is shown in the topmost spectra, also in Figs. 9b and 10b.

For all spectra in Figs. 9 and 10, a broad peak appeared in the wave number region 2500–3800 cm^{-1}, corresponding to the vibrational frequencies of various surface hydroxyl species. Considering PdAl, a prominent, negative peak with minimum at around 3534 cm^{-1} for PdAl and 3549 cm^{-1} for PdAl-2Ba was slowly developed in the O_2/Ar flow after water exposure, see Figs. 9a and 10a. This peak was weakly visible already after 5 min, however the gradual growth during 120 min indicates slow dehydroxylation. The same corresponding peak, at around 3534 cm^{-1} for PdAl and 3549 cm^{-1} for PdAl-2Ba, also appeared during water adsorption, see bottom spectra in Figs. 9b and 10b. In these figures it can be seen that most of the hydroxyl formation occurred
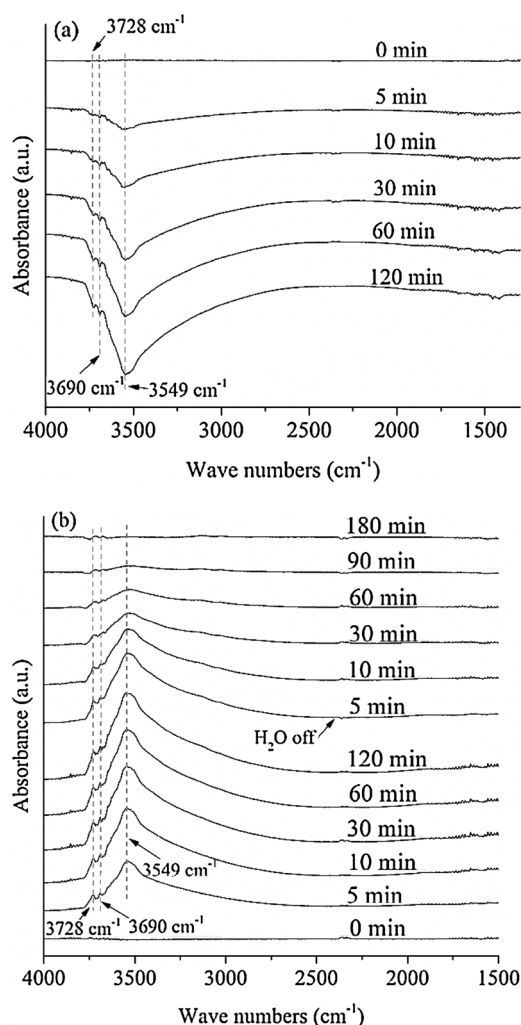
Fig. 10. *In situ* DRIFTS spectra for desorption/adsorption of water/hydroxyls on the surface of PdAl-2Ba at 550 °C. The spectra were collected during (a) 120 min O$_2$/Ar purge after H$_2$O$_g$/O$_2$/Ar exposure, the background was acquired with presence of H$_2$O$_g$/O$_2$ and (b) during 120 min H$_2$O$_g$/O$_2$/Ar exposure followed by 180 min of O$_2$/Ar purge, the background was acquired with presence of O$_2$.

hydroxyls adsorbed upon Al$_2$O$_3$ when Pd/Al$_2$O$_3$ was provided with a water vapor containing gas feed. However, this latter mentioned absorbance band might arise from hydroxyls on the interface of Pd-Al$_2$O$_3$ rather than on the Al$_2$O$_3$ support, which was discussed in the paper by Schwartz et al. [13]. The samples (PdAl and PdAl-2Ba) tested in our experiment, can be expected to exhibit common peaks for hydroxyls formed on PdO, the Al$_2$O$_3$ support and the interface between Pd-Al$_2$O$_3$ whereas differences can arise from the hydroxyls formed upon Ba and the interface of Ba-Pd and Ba-Al$_2$O$_3$ on the PdAl-2Ba sample. The fact that no significant difference in peak position could be seen for PdAl and PdAl-2Ba implies that only small amounts of hydroxyls are formed on the Ba or the interface of Ba compared to on PdO and Al$_2$O$_3$ and could therefore not be distinguished due to the large amount of other surface hydroxyls.

As discussed previously, the flow reactor experiments showed that the CH$_4$ oxidation in the presence of water vapor was enhanced by an addition of Ba to Pd/Al$_2$O$_3$. It was also observed that the addition of Ba to Pd/Al$_2$O$_3$ facilitates regeneration of the catalytic activity after water deactivation. However, the DRIFTS experiments did not give any indications of faster water desorption or less extensive surface hydroxyl formation upon PdAl-2Ba. However, it is possible that the low Ba concentration results in weak intensity of for instance Ba(OH)$_2$, which therefore will not be distinguishable in the IR absorbance spectra. Thus, it is possible that hydroxyl formation on Ba and on the interface of Ba-Pd and/or Ba-Al$_2$O$_3$ changes the surface chemistry of the Ba promoted samples and that the addition of Ba therefore impacts the water deactivation and regeneration.

4. Conclusions

Pd/Al$_2$O$_3$ becomes severely deactivated in the presence of water vapor, resulting in low CH$_4$ conversion. We have therefore studied the addition of barium to Pd/Al$_2$O$_3$, with a special emphasis on the deactivation and regeneration by water. The catalyst samples were characterized thoroughly using temperature programmed oxidation (TPO), temperature programmed reduction with CH$_4$ (CH$_4$-TPR), X-ray photoelectron spectroscopy (XPS), scanning transmission electron microscopy (STEM) and *in situ* diffuse reflectance infrared Fourier transform spectroscopy (*in situ* DRIFTS).

In this study, we have shown that an addition of Ba increases the resistance towards water deactivation. This was observed in flow reactor experiments where the Ba promoted samples showed both milder and delayed water deactivation compared to unpromoted Pd/Al$_2$O$_3$. We also showed that a higher degree of regeneration after water deactivation could be obtained by an addition of Ba to Pd/Al$_2$O$_3$, particularly at lower regeneration temperatures such as 600 °C and 500 °C. Thus, an addition of Ba to Pd/Al$_2$O$_3$ mitigates the water deactivation effect and facilitates the regeneration of the CH$_4$ oxidation activity after water vapor exposure. Analysis with TPO, CH$_4$-TPR and XPS gave no evidence for that electronic promotion of the CH$_4$ oxidation activity was provided from an addition of up to 2 wt.% Ba. Using DRIFT-spectroscopy, we observed that there were no differences on the adsorption/desorption rate for water/hydroxyl species for the unpromoted and promoted samples. It is likely that the reason was that it was difficult to distinguish the IR absorbance peaks of hydroxyls formed on Ba due to the high IR absorbance of other hydroxyl species on PdO and Al$_2$O$_3$.

To conclude, our results clearly shows that it is not only the interaction between the palladium sites and water that plays a role, but also that the support is important. Moreover, the addition of barium to Pd/Al$_2$O$_3$ is beneficial for methane oxidation, since it lowers the rate for water inhibition and at the same time facilitates easier regeneration.

Acknowledgement

rapidly within the first 10 min. It should also be noted that the slowly proceeded water desorption can be seen in the topmost spectra in Figs. 9b and 10b as well. Thus, the adsorption of water occurred rather quickly, whereas the hydroxyl desorption proceeded more slowly. No significant difference in water adsorption or desorption rate could be seen for PdAl and PdAl-2Ba in these experiments.

Ciuparu et al. [37] associated the absorption bands in the wavenumber regions 3732, 3699 and 3549 cm^{-1} to hydroxyl species formed on the surface of PdO and its interface towards the alumina support. These wavenumbers were suggested to correspond to terminal, bridged and multi-bound hydroxyls, respectively, and have also been reported by other authors [12,17]. Absorbance peaks in the similar wave number regions can be seen in Figs. 9 and 10, thus the peaks at 3728 cm^{-1} and 3690 cm^{-1} for PdAl and PdAl-2Ba are assigned to terminal and bridged hydroxyls on PdO and the interface of PdO-Al$_2$O$_3$, respectively. The broad peak at 3534 cm^{-1} for PdAl and 3549 cm^{-1} for PdAl-2Ba corresponds to multi-bound hydroxyls. Undoubtedly, extensive hydroxyl formation also occurs upon the surface of the Al$_2$O$_3$ support. Previous DRIFTS studies have ascribed absorption peaks at 3680, 3723 and 3770 cm^{-1} to hydroxyl species on bare γ-Al$_2$O$_3$ [37,38]. Some authors have reported that these peaks have considerably lower intensity than the hydroxyls formed on Pd and are not likely to be distinguishable [17,37], whereas Gao et al.[12] ascribed a broad band at 3445 cm^{-1} to

Appendix A. Supplementary data

Supplementary material related to this article can be found, in the online version, at doi:https://doi.org/10.1016/j.apcatb.2018.03.003.

References

[1] P. Gelin, M. Primet, Complete oxidation of methane at low temperature over noble metal based catalysts: a review, Appl. Catal. B Environ. 39 (2002) 1–37.

[2] R. Gholami, M. Alyani, K.J. Smith, Deactivation of Pd catalysts by water during low temperature methane oxidation relevant to natural gas vehicle converters, Catalysts 5 (2015) 561–594.

[3] M. Lyubovsky, L. Pfefferle, Methane combustion over the alpha-alumina supported Pd catalyst: activity of the mixed Pd/PdO state, Appl. Catal. A Gen. 173 (1998) 107–119.

[4] J. Nilsson, P.A. Carlsson, S. Fouladvand, N.M. Martin, J. Gustafson, M.A. Newton, E. Lundgren, H. Gronbeck, M. Skoglundh, Chemistry of supported palladium nanoparticles during methane oxidation, ASC Catal. 5 (2015) 2481–2489.

[5] S.W. Yang, A. Maroto-Valiente, M. Benito-Gonzalez, I. Rodriguez-Ramos, A. Guerrero-Ruiz, Methane combustion over supported palladium catalysts I. Reactivity and active phase, Appl. Catal. B Environ. 28 (2000) 223–233.

[6] R. Burch, F.J. Urbano, Investigation of the active state of supported palladium catalysts in the combustion of methane, Appl. Catal. A Gen. 124 (1995) 121–138.

[7] M. Lyubovsky, L. Pfefferle, Complete methane oxidation over Pd catalyst supported on alpha-alumina. Influence of temperature and oxygen pressure on the catalyst activity, Catal. Today 47 (1999) 29–44.

[8] T.V. Choudhary, S. Banerjee, V.R. Choudhary, Catalysts for combustion of methane and lower alkanes, Appl. Catal. A Gen. 234 (2002) 1–23.

[9] R. Burch, F.J. Urbano, P.K. Loader, Methane combustion over palladium catalysts: the effect of carbon dioxide and water on activity, Appl. Catal. A Gen. 123 (1995) 173–184.

[10] C.F. Cullis, T.G. Nevell, D.L. Trimm, Role of the catalyst support in the oxidation of methane over palladium, J. Chem. Soc. Faraday Trans. 1 68 (1972) 1406–1412.

[11] R. Kikuchi, S. Maeda, K. Sasaki, S. Wennerstrom, K. Eguchi, Low-temperature methane oxidation over oxide-supported Pd catalysts: inhibitory effect of water vapor, Appl. Catal. A Gen. 232 (2002) 23–28.

[12] D.N. Gao, S. Wang, C.X. Zhang, Z.S. Yuan, S.D. Wang, Methane combustion over Pd/Al2O3 catalyst: effects of chlorine ions and water on catalytic activity, Chin. J. Catal. 29 (2008) 1221–1225.

[13] W.R. Schwartz, D. Ciuparu, L.D. Pfefferle, Combustion of methane over palladium-based catalysts: catalytic deactivation and role of the support, J. Phys. Chem. C 116 (2012) 8587–8593.

[14] W.R. Schwartz, L.D. Pfefferle, Combustion of methane over palladium-based catalysts: support interactions, J. Phys. Chem. C 116 (2012) 8571–8578.

[15] N. Sadokhina, F. Ghasempour, X. Auvray, G. Smedler, U. Nylén, M. Olofsson, L. Olsson, An experimental and kinetic modelling study for methane oxidation over Pd-based catalyst: inhibition by water, Catal. Lett. 147 (2017) 2360–2371.

[16] O. Mihai, G. Smedler, U. Nylén, M. Olofsson, L. Olsson, The effect of water on methane oxidation over Pd/Al2O3 under lean, stoichiometric and rich conditions, Catal. Sci. Technol. 7 (2017) 3084–3096.

[17] K. Persson, L.D. Pfefferle, W. Schwartz, A. Ersson, S.G. Jaras, Stability of palladium-based catalysts during catalytic combustion of methane: the influence of water, Appl. Catal. B Environ. 74 (2007) 242–250.

[18] D. Roth, P. Gelin, M. Primet, E. Tena, Catalytic behaviour of Cl-free and Cl-containing Pd/Al2O3 catalysts in the total oxidation of methane at low temperature, Appl. Catal. A Gen. 203 (2000) 37–45.

[19] X. Auvray, A. Lindholm, M. Miroslawa, L. Olsson, The addition of alkali and alkaline earth metals to Pd/Al2O3 to promote methane combustion. Effect of Pd and Ca loading, Catal. Today 299 (2017) 212–218.

[20] F. Klingstedt, H. Karhu, A.K. Neyestanaki, L.E. Lindfors, T. Salmi, J. Vayrynen, Barium promoted palladium catalysts for the emission control of natural gas driven vehicles and biofuel combustion systems, J. Catal. 206 (2002) 248–262.

[21] P.O. Thevenin, E. Pocoroba, L.J. Pettersson, H. Karhu, I.J. Vayrynen, S.G. Jaras, Characterization and activity of supported palladium combustion catalysts, J. Catal. 207 (2002) 139–149.

[22] H. Shinjoh, N. Isomura, H. Sobukawa, M. Sugiura, Effect of alkaline addition on hydrocarbon oxidation activities of palladium three-way catalyst, Stud. Surf. Sci. Catal. 116 (1998) 83–91.

[23] L.F. Liotta, G. Deganello, Thermal stability, structural properties and catalytic activity of Pd catalysts supported on Al2O3-CeO2-BaO mixed oxides prepared by sol-gel method, J. Mol. Catal. A Chem. 204 (2003) 763–770.

[24] C.G. Vayenas, S. Bebelis, C. Pilangos, S. Brosda, D. Tsiplakides, Electrochemical Activation of Catalysis: Promotion, Electrochemical Promotion, and Metal-Support Interactions, Kluwer Academic/Plenum Publishers, New York, 2001.

[25] H. Arai, M. Machida, Thermal stabilization of catalyst supports and their application to high-temperature catalytic combustion, Appl. Catal. A Gen. 138 (1996) 161–176.

[26] M.F.M. Zwinkels, S.G. Jaras, P.G. Menon, T.A. Griffin, Catalytic materials for high-temperature combustion, Catal. Rev. Sci. Eng. 35 (1993) 319–358.

[27] N. Sadokhina, G. Smedler, U. Nylen, M. Olofsson, L. Olsson, The influence of gas composition on Pd-based catalyst activity in methane oxidation - inhibition and promotion by NO, Appl. Catal. B Environ. 200 (2017) 351–360.

[28] P. Castellazzi, G. Groppi, P. Forzatti, E. Finocchio, G. Busca, Activation process of Pd/Al2O3 catalysts for CH4 combustion by reduction/oxidation cycles in CH4-containing atmosphere, J. Catal. 275 (2010) 218–227.

[29] K. Otto, L.P. Haack, J.E. Devries, Identification of two types of oxidized palladium on gamma-alumina by X-ray photoelectron spectroscopy, Appl. Catal. B Environ. 1 (1992) 1–12.

[30] R.J. Bird, P. Swift, Energy calibration in electron spectroscopy and the re-determination of some reference electron binding energies, J. Electron Spectrosc. Relat. Phenom. 21 (1980) 227–240.

[31] D.H. Kim, S.I. Woo, J.M. Lee, O.B. Yang, The role of lanthanum oxide on Pd-only three-way catalysts prepared by co-impregnation and sequential impregnation methods, Catal. Lett. 70 (2000) 35–41.

[32] K.S. Kim, A.F. Gossmann, N. Winograd, X-ray photoelectron spectroscopy studies of palladium oxides and the palladium-oxygen electrode, Anal. Chem. 46 (1974) 197–200.

[33] K. Persson, K. Jansson, S.G. Jaras, Characterisation and microstructure of Pd and bimetallic Pd-Pt catalysts during methane oxidation, J. Catal. 245 (2007) 401–414.

[34] L.S. Kibis, A.I. Titkov, A.I. Stadnichenko, S.V. Koscheev, A.I. Boronin, X-ray photoelectron spectroscopy study of Pd oxidation by RF discharge in oxygen, Appl. Surf. Sci. 255 (2008) 9248–9254.

[35] X.Y. Zhang, E.Y. Long, Y.L. Li, L.J. Zhang, J.X. Guo, M.C. Gong, Y.Q. Chen, The effect of CeO2 and BaO on Pd catalysts used for lean-burn natural gas vehicles, J. Mol. Catal. A Chem. 308 (2009) 73–78.

[36] K. Persson, A. Ersson, K. Jansson, N. Iverlund, S. Jaras, Influence of co-metals on bimetallic palladium catalysts for methane combustion, J. Catal. 231 (2005) 139–150.

[37] D. Ciuparu, E. Perkins, L. Pfefferle, In situ DR-FTIR investigation of surface hydroxyls on gamma-Al2O3 supported PdO catalysts during methane combustion, Appl. Catal. A Gen. 263 (2004) 145–153.

[38] S.S. Deshmukh, V.I. Kovalchuk, V.Y. Borovkov, J.L. d'Itri, FTIR spectroscopic and reaction kinetics study of the interaction of CF3CFCl2 with gamma-Al2O3, J. Phys. Chem. B 104 (2000) 1277–1284.